

UCSF

UC San Francisco Previously Published Works

Title

Antiretroviral Therapy Concentrations Differ in Gut vs. Lymph Node Tissues and Are Associated With HIV Viral Transcription by a Novel RT-ddPCR Assay.

Permalink

<https://escholarship.org/uc/item/9914c5t5>

Journal

JAIDS Journal of Acquired Immune Deficiency Syndromes, 83(5)

ISSN

1525-4135

Authors

Lee, Sulggi A  
Telwatte, Sushama  
Hatano, Hiroyu  
et al.

Publication Date

2020-04-15

DOI

10.1097/qai.0000000000002287

Peer reviewed



Published in final edited form as:

*J Acquir Immune Defic Syndr.* 2020 April 15; 83(5): 530–537. doi:10.1097/QAI.0000000000002287.

## Antiretroviral therapy concentrations differ in gut versus lymph node tissues and are associated with HIV viral transcription by a novel RT-ddPCR assay

Sulggi A. Lee<sup>1,a</sup>, Sushama Telwatte<sup>1,2,a</sup>, Hiroyu Hatano<sup>1</sup>, Angela D.M. Kashuba<sup>3</sup>, Mackenzie L. Cottrell<sup>3</sup>, Rebecca Hoh<sup>1</sup>, Teri J. Liegler<sup>1</sup>, Sophie Stephenson<sup>1</sup>, Ma Somsouk<sup>4</sup>, Peter W. Hunt<sup>5</sup>, Steven G. Deeks<sup>1</sup>, Steven Yukl<sup>1,2,b</sup>, Radojka M. Savic<sup>6,b</sup>

<sup>1</sup>University of California San Francisco, Department of Medicine, Division of Infectious Diseases, HIV, and Global Medicine

<sup>2</sup>San Francisco VA Medical Center (SFVAMC), San Francisco, CA, USA

<sup>3</sup>University of North Carolina, Eschelman School of Pharmacy, Division of Pharmacotherapy and Experimental Therapeutics

<sup>4</sup>University of California San Francisco, Department of Medicine, Division of Gastroenterology

<sup>5</sup>University of California San Francisco, Department of Medicine, Division of Experimental Medicine

<sup>6</sup>University of California San Francisco, Department of Bioengineering and Therapeutic Sciences

### Abstract

**Background:** The majority of HIV-infected cells during antiretroviral therapy (ART) persist in lymphoid tissues. Studies disagree on whether suboptimal tissue ART concentrations contribute to ongoing HIV replication during viral suppression.

**Methods:** We performed a cross-sectional study in virally-suppressed HIV+ participants measuring lymphoid tissue ART (darunavir [DRV], atazanavir [ATV], and raltegravir [RAL]) concentrations by LC-MS/MS assay. Tissue and plasma ART concentrations were used to estimate tissue:plasma penetration ratios (TPRs) as well as drug-specific tissue:inhibitory concentration

**Corresponding author:** Sulggi A. Lee, M.D., PhD., University of California San Francisco, Department of Medicine, Division of HIV/AIDS, 995 Potrero Avenue, Building 80, Box 0874, San Francisco, CA 94110, Tel: (415) 735-5127, Fax: (415) 476-6953, sulggi.lee@ucsf.edu. **Alternate corresponding author:** Radojka M. Savic, Ph.D., University of California San Francisco, Department of Bioengineering and Therapeutic Sciences, 1550 4th Street, Building 19B, Box 2911, San Francisco, CA 94158, Tel: (415) 502-0640, Fax: (415) 514-4361, rada.savic@ucsf.edu. **Reprints:** Reprint requests can be directed to Dr. Sulggi Lee, the corresponding author (contact information above).

<sup>a</sup>Co-primary authors

<sup>b</sup>Co-senior authors

#### AUTHOR CONTRIBUTIONS

HH and SAL designed the study and acquired funding, with supplemental funding from SGD and RMS. HH, SAL, RH, PWH, and SGD coordinated the collection, management, and quality control processes for the clinical data and specimens, including the colonoscopy procedures performed by MS. TJL and SS provided specimen handling and storage support. MLC and ADK performed the pharmacologic assays. ST and SY conducted the HIV RNA and DNA quantification assays. SAL, MLC, and RMS analyzed the data. SAL wrote the report with critical feedback from MLC, ST, and SY and the other co-authors to finalize the report.

**CONFLICTS:** The authors do not have a commercial or other association that might pose a conflict of interest.

**Previous presentation:** Preliminary data were presented in February 2017, as an oral presentation at the Conference on Retroviruses and Opportunistic Infections (CROI) in Seattle, WA, Abstract number 407.

ratios (TICs). HIV DNA and sequentially-produced HIV RNA transcripts were quantified from rectal biopsies using droplet digital PCR (ddPCR) assays.

**Results:** Tissue samples were collected in duplicate from 19 participants: 38 rectal, 8 ileal (4 RAL, 2 DRV, 2 ATV), and 6 lymph node (4 RAL, 2 DRV) samples. Overall, median TICs were higher for RAL than DRV or ATV (both  $P=0.006$ ). Median TICs were lower in lymph nodes vs. ileum (0.49 vs. 143,  $P=0.028$ ) or rectum (33,  $P=0.019$ ), and all ART levels were below target concentrations. Higher rectal TICs were associated with lower HIV RNA transcripts (read-through, long LTR, and Nef,  $P$  all  $<0.026$ ) and a lower long LTR RNA/long LTR DNA ratio ( $P=0.021$ ).

**Conclusions:** We observed higher tissue ART concentrations in ileum and rectum compared to lymph nodes. We observed higher HIV transcription in participants with lower rectal ART concentrations. These findings add to the limited data supporting the idea that viral transcription may be influenced by ART concentrations in lymphoid tissues. Further exploration of tissue pharmacokinetics is needed in future HIV eradication strategies.

### Keywords

antiretroviral therapy; pharmacokinetics; pharmacodynamics; HIV transcription; lymphoid tissue

## INTRODUCTION

Persistent HIV despite effective antiretroviral therapy (ART) may contribute to the “HIV reservoir”<sup>1</sup> and drive high levels of immune activation and increased mortality rates in HIV+ compared to HIV-negative individuals.<sup>2,3</sup> The majority of persistently HIV-infected cells are in lymphoid tissues.<sup>4</sup> Whether or not suboptimal ART concentrations in lymphoid tissues contribute to residual viral replication during ART has been strongly debated. Some ART intensification studies in which a fourth drug (e.g., raltegravir, RAL) is added to an existing suppressive ART regimen demonstrated support for ongoing viral transcription,<sup>5,6</sup> but others studies have not.<sup>7-10</sup> Though some studies found evidence of lower ART concentrations in lymphoid tissues to be associated with increased viral transcription and evolution,<sup>11,12</sup> a recent study using *in situ* ART quantification methods<sup>13</sup> found no association between concentrations of integrase inhibitors (raltegravir [RAL] and dolutegravir [DTG]) and copies of HIV total DNA or unspliced RNA in rectal tissue by droplet digital PCR (ddPCR).<sup>14</sup>

ART concentrations have also been shown to be lower in lymphoid tissues than in plasma,<sup>11,12</sup> lower in lymph node than in gut-associated lymphoid tissue (GALT),<sup>12</sup> and among gut tissues, lower in rectal than in ileal tissue.<sup>15</sup> These findings are somewhat difficult to interpret, as prior studies have used different methods to quantify ART concentrations in tissue. Two prominent methods include quantifying ART from tissue homogenates<sup>15</sup> versus from extracted mononuclear cells.<sup>12,16</sup> The former method may overestimate ART concentrations due to homogenization of whole biopsy tissues (which might contain ART in non-lymphoid cells)<sup>17</sup> while the latter method may underestimate ART concentrations (ART cell permeability and processing steps can lead to reduced intracellular concentrations).<sup>18</sup> In addition, ART regimens may have differential lymphoid tissue penetration. RAL, an integrase inhibitor (INI) had superior concentrations in rectal tissue compared to other drugs

(protease inhibitors [PIs], nucleoside reverse transcriptase inhibitors [NRTIs], non-nucleoside reverse transcriptase inhibitors [NNRTIs], and CCR5 inhibitors),<sup>19</sup> and higher rectal concentrations than DTG, another INI.<sup>13,20</sup>

We performed a cross-sectional study of HIV+ ART-suppressed individuals treated during chronic or early HIV infection. Tissue ART pharmacokinetics were measured in homogenates of rectal, ileal, and lymph node samples using validated liquid chromatography-mass spectrometry (LC-MS) methods compared to copies of HIV DNA and RNA using ddPCR assays that captured specific sequential stages of HIV transcription.

## METHODS

### Study participants

HIV-infected adults from the University of California San Francisco (UCSF) SCOPE cohort were consented to undergo a rectal biopsy; a subset also consented to optional ileal and lymph node sampling. Inclusion criteria were confirmed HIV-1 infection, viral suppression for 12 months on initial ART regimen, and plasma HIV RNA <40 copies/mL. Participants were included if they were taking oral (1) RAL 400 mg daily + emtricitabine/tenofovir disoproxil fumarate (TDF/FTC) bid, (2) atazanavir (ATV) 300 mg daily + ritonavir 100 mg daily + TDF/FTC daily, or (3) darunavir (DRV) 800 mg daily + ritonavir 100 mg daily + TDF/FTC daily. Major exclusion criteria were pregnant or breastfeeding women, a history of a blood coagulation disorder, inflammatory colitis, recent serious illness requiring hospitalization, recent vaccination, and recent use of immunodulatory drugs. Additional exclusion criteria for lymph node biopsy were a history of inguinal skin infection, lower extremity venous stasis, and cancer of the lower extremity. All participants provided written informed consent, and the institutional review board of UCSF approved the research.

### Sampling procedures

All participants underwent rectal sampling, with removal of up to 30 3-mm biopsies. Ileal biopsies were collected in a subset of participants who consented to a colonoscopy (using similar sampling methods). For rectal and ileal sampling, 10–12 biopsy pieces were immediately flash-frozen and stored at –80°C. Four to 6 gut biopsy pieces were analyzed for ART concentrations,<sup>21,22</sup> while another 6 pieces were analyzed for cellular HIV RNA and DNA.<sup>23</sup> For optional lymph node sampling, a single inguinal lymph node was carefully excised and dispersed to a single cell suspension, flash-frozen, and sent for tissue pharmacokinetic analysis.<sup>24–26</sup>

### Antiretroviral quantification (plasma, GALT, and lymph nodes)

RAL, DRV, and ATV concentrations were quantified by validated LC-MS/MS methods. Whole tissue biopsies were weighed and homogenized in Precellys® tubes (Cayman Chemicak, MI, USA), analytes were extracted from tissue homogenate and plasma samples by protein precipitation with isotopically labeled internal standards and then detected on an API-5000 Triple Quad mass spectrometer (AB SCIEX, Foster City, CA, USA). Calibration standards and quality control samples were within 20% of nominal values with the following

dynamic ranges: 1–10,000ng/ml of tissue homogenate (ATV, DRV and RAL), 5–5000ng/ml of plasma (raltegravir), and 50–20,000ng/ml of plasma (ATV, and DRV).

### HIV RNA and DNA quantification (GALT)

A novel panel of reverse transcription (RT)-ddPCR assays was performed to quantify HIV RNAs produced during sequential stages of viral transcription.<sup>23</sup> Intact flash frozen rectal biopsies (6 pieces) were homogenized and total cellular RNA and DNA were isolated from homogenized rectal cells using Trireagent (Molecular Research Center).<sup>23</sup> HIV DNA (Long LTR) and sequential steps in HIV RNA transcription were quantified from rectal biopsies using RT-ddPCR assays (Bio-Rad QX100 Droplet Digital qPCR System) reflecting HIV transcriptional interference (“read-through”), transcriptional initiation (TAR), elongation (“Long LTR”), distal transcription (Nef), completion (“PolyA”), and multiple splicing (Tat-Rev) events.<sup>23</sup> HIV DNA was measured under the same ddPCR conditions and using the same primers and probes used to measure each HIV RNA. The total cell equivalents (for normalizing the frequency of DNA and RNA copies) were determined by measuring the absolute copy numbers of a nonduplicated cellular gene, Telomere Reverse Transcriptase (*TERT*), in the extracted cellular DNA by ddPCR.<sup>23,27</sup>

### Statistical Methods

Ileal, rectal, and lymph node ART concentrations were calculated as tissue:plasma penetration ratios (TPRs)<sup>15</sup> by first converting tissue concentrations to ng/mL (assuming a tissue density of 1.06 g/mL<sup>28</sup>) and then dividing the tissue concentration by the plasma concentration for each tissue type. A TPR=1 indicated equal tissue and plasma ART concentrations. Drug-specific *in vivo* inhibitory concentrations<sup>29,30</sup> were also used to estimate tissue concentration:inhibitory ratios (TICs) as clinically relevant measures of PK to be analyzed along with TPRs. Wilcoxon rank sum tests were used to compare median TPRs/TICs.

Exploratory analyses to simulate time-dependent PK profiles from our cross-sectional data were performed. Using nonlinear mixed effects models, drug concentrations over time were estimated for each tissue and each ART type using compartmental plasma-tissue PK analyses in NONMEM (version 7.3; Icon Development Solutions, Dublin, Ireland). Monte Carlo simulations were performed incorporating self-reported time of last ART dose and previously published plasma PK data for each drug.<sup>31–33</sup> Simulated TPRs were calculated as a fraction of plasma exposure (tissue area under the curve [AUC] ÷ plasma AUC) for each biologic duplicate and compared to target plasma *in vivo* concentrations below which virologic failure had been reported in clinical trials.<sup>29,30</sup>

For the PD analysis, negative binomial regression models<sup>34</sup> were fit to assess the effects of tissue PK (TPR or TIC) on HIV copies and HIV RNA/DNA ratios. The number of HIV copies was modeled as the outcome variable and the number of input cells as the offset (exposure) variable. To evaluate HIV RNA/DNA ratios, mixed effects models were fit with an interaction term for PK and HIV copies. By specifying the HIV targets (e.g., TAR RNA and Long LTR DNA, for example), the interaction term estimated the fold-change in HIV RNA/DNA per unit change in TPR (or TIC). Multivariate regressions were performed

including covariates for age, gender, nadir CD4+ T cell count, maximum pre-ART HIV RNA, recent CD4+ T cell count, early ART initiation (within 6 months of estimated date of infection), duration of ART suppression, and ART regimen (PI vs. INI). Similar models were fit for evaluating ART regimen (PI=1 vs. INI=0) as the predictor variable with HIV copies or HIV RNA/DNA ratio as the outcome variable.

## RESULTS

Participants were mostly male, with a median age of 44 years, nadir CD4+ T cell count of 304 cells/mm<sup>3</sup>, pre-ART HIV RNA of 5.3 log<sub>10</sub>copies/mL, recent CD4+ T cell count of 642 cells/mm<sup>3</sup>, and duration of ART suppression of 4 years (Table S1). Four participants had initiated ART within approximately 6 months of HIV infection (range from 2.0 to 4.9 months).

PK measures (TPRs and TICs) were relatively consistent between biologic duplicates (median intra-assay coefficient of variation=21%) (Figure 1). Median PK measures were non-statistically significantly higher in ileum compared to rectum (TPR: 8.13 vs. 2.85; TIC: 143 vs. 33) and statistically significantly lower in lymph nodes compared to ileum (TPR=0.22 vs. 8.13, P=0.0019; TIC=0.49 vs. 143, P=0.028) and lower in lymph nodes compared to rectum (TPR=0.22 vs. 2.85, P=0.0001; TIC: 0.49 vs. 33, P=0.019) (Figure 1). While median TPRs were not statistically significantly different by ART regimen (PI vs. INI from rectal, ileal, or lymph node tissues), median TICs in rectal tissue were statistically significantly higher for INI vs. PI regimens (RAL=109 vs. ATV=25 [P=0.0061] or vs. DRV=15 [P=0.0059]). There were no statistically significant differences in median rectal TPRs or TICs by timing of ART (2 participants on RAL- and 2 participants on DRV-based regimens; data not shown).

We also performed compartmental PK analyses to estimate ART pharmacokinetics over time using our cross-sectional data and incorporating previously published plasma PK data<sup>31–33</sup> for each drug (Figure S1–S2). Final PK parameters were estimated for each drug, including the ratio of plasma to tissue concentrations accounting for time from last ART dose ( $r_{pl-tissue}$ ) (Table S2). Due to limited data available, the rate constant of drug concentration from plasma to tissue and vice versa ( $k_{pl-tissue}$ ) was fixed to a low or high value, dependent on the sensitivity analysis performed. These models demonstrated that one participant taking DRV had plasma and tissue (rectal, ileal, and lymph node) DRV concentrations that fell below the target plasma inhibitory concentration (IC),<sup>30</sup> suggesting that this participant had suboptimal/missed dosing prior to sample collection (Figure 2A). In contrast, although all participants taking RAL and had plasma concentrations above the RAL target plasma IC, two participants had lymph node samples below the target IC (Figure 2C).<sup>29</sup> Comparison across tissues was possible for RAL since all tissue types (rectal, ileal, lymph node, and plasma) were collected; predicted RAL PK profiles demonstrated that RAL concentrations remained above the target inhibitory concentrations in all tissues except lymph nodes (Figure 2C).

Finally, we performed PD analyses by quantifying HIV RNA from rectal tissue in 10 of the 19 participants and HIV Long LTR DNA in all 19 participants (Tables 1–2, S3–S4). There

was an overall inverse relationship between PK measures and copies of HIV (RNA or RNA/DNA ratios). There were statistically significantly lower Long LTR RNA/Long LTR DNA ratios per two-fold increase in TPR (0.22-fold lower,  $P=0.04$ ) or TIC (0.36-fold lower,  $P=0.021$ ). There were also statistically significant lower frequencies of HIV RNA copies of Readthrough (0.56-fold lower,  $P=0.026$ ), Long LTR (0.25-fold lower,  $P=0.014$ ), and Nef (0.20-fold lower,  $P=0.044$ ) for each two-fold increase in TIC (Table 2). These associations persisted after controlling for age, nadir CD4+ T cell count, pre-ART HIV RNA, recent CD4+ T cell count, duration of ART suppression, ART regimen (PI vs. INI) and early ART initiation (Tables S5–S6). In three individuals with ileal data, we observed a similar trend between TPR and copies of Long LTR DNA (0.85-fold lower,  $P=0.046$ ) but this was based on only three observations and a similar trend was not observed with TIC (Figure S3). HIV RNA data were not available from the lymph node samples.

Participants on PI-based regimens had slightly lower median nadir CD4+ T cell count (312 vs. 432 cells/mm<sup>3</sup>), higher pre-ART log<sub>10</sub>HIV RNA (5.4 vs. 5.3 copies/mL), and were less likely to have initiated ART early (14% vs. 67%). Although based on small numbers of participants taking ART regimens containing PIs (N=7–11) vs. INIs (N=2–8), there were generally higher frequencies of HIV RNA (and similar trends with RNA/DNA ratios) for participants on PI- vs. INI-based regimens (Table 3).

## DISCUSSION

Our findings add to the limited literature evaluating tissue ART concentrations and residual viral replication.<sup>6,11–13</sup> Here, we used cross-sectional samples from HIV+ ART-suppressed individuals to compare differences in ART concentrations by tissue (rectum, ileum, lymph node) and by ART regimen (PI vs. INI). We observed higher tissue PK in ileal and rectal compared to lymph node tissues and observed a statistically significant association between higher tissue PK (TPR and TIC) and lower levels of viral transcription (HIV RNA and RNA/DNA ratios). We observed no differences in tissue PK by ART regimen when quantified by TPR or compartmental PK modeling, but we did observe higher tissue TICs for INI vs. PI-based regimens. Since we also observed higher viral transcription with PI vs. INI-based regimens, this suggests potential PK as well as non-pharmacologic factors associated with ART regimen in influencing viral transcription. Clinically, these findings suggest that efforts to enhance tissue ART concentrations may be important for preventing HIV transmission (e.g., preexposure prophylaxis) and/or reducing potential residual HIV transcription (i.e., HIV persistence in tissues). Additional dose-finding studies may help elucidate why RAL<sup>19,20</sup> (but not DTG<sup>13</sup>) compared to PI-based regimens appear to be associated with higher tissue concentrations and lower viral transcription.

Consistent with prior data,<sup>15</sup> using the same LC-MS method, we found that ART concentrations were slightly higher in ileal vs. rectal tissue, but these associations were not statistically significant. Similar to a prior report using a different method,<sup>12</sup> we did observe statistically significantly higher tissue ART concentrations in rectum and ileum vs. lymph nodes. Using compartmental PK analyses to estimate the time above target viral IC for each drug,<sup>29,30</sup> for individuals taking RAL, we were able to compare across all three tissue types. RAL levels were above target in plasma, rectal, and ileal tissues but not in lymph nodes for

one participant. Further studies are needed to determine the proportion of participants who may have concentrations below the IC as our analyses were based on simulations from cross-sectional data from very few participants.

We observed that higher ART concentrations were associated with statistically significant fold-reductions in viral transcription using a novel ddPCR-based assay quantifying sequential HIV transcripts.<sup>23</sup> Our data support prior work demonstrating evidence of viral evolution in lymphoid tissues in 5 individuals who were treated during acute infection and sampled during the first 6 months of ART suppression<sup>11</sup> but are in contrast to reports finding no evidence of viral evolution in tissues of HIV+ ART-suppressed individuals initiating ART during chronic infection with prolonged duration of ART.<sup>35–39</sup> Potential reasons for the discrepancy in these studies may include differences in the duration of ART suppression and/or the timing of ART initiation in these individuals, which could affect the strength of the immune response and subsequent effects on residual viral transcription and replication in lymphoid tissues,<sup>37,40–42</sup> as well as differences in the sensitivity of the HIV assays.<sup>23</sup> Our findings also differ from a recent study evaluating RAL and DTG concentrations in rectal tissue, which found no association with HIV unspliced RNA or total DNA.<sup>13</sup>

We observed higher levels of HIV RNA in the rectum of participants on PI- vs. INI-based regimens. These findings could be due to the higher tissue PK for RAL than DRV or ATV, as measured by TIC (Figure 1B). However, by TPR or by compartmental PK modeling, we did not observe a significant difference in tissue PK by ART regimen. Thus, differences in viral replication may be due to PK as well as non-PK factors. Yet, none of the ART regimens included in our study are known to affect reactivation from latency or to block HIV transcription (except insofar as they inhibit new infections), but lower ART concentrations might allow progression through parts of the viral lifecycle (or even one cycle) without multiple rounds of ongoing replication. The findings might potentially relate to the different stages of the viral lifecycle that are blocked by these drugs. Since integrase inhibitors block the last step prior to latency or viral transcription, whereas PIs act after viral particle release, integrase inhibitors may have a mechanistic advantage over PIs in limiting the frequency of integrated HIV, and hence transcription, in tissues. Alternatively, protease inhibitors, which have been shown to directly inhibit apoptosis in animal models,<sup>43</sup> might actually favor the survival of transcriptionally active HIV-infected cells (potentially by enhancing mitochondrial stability), leading to further induction of viral transcription.

It should be noted that our PD analyses included only three individuals on INI-based ART. Given the limited number of participants in each ART group from our cross-sectional study, additional studies including more patients and more sensitive *in situ* ART quantification methods<sup>13</sup> may be required to adequately compare tissue exposure and effects of different ART regimens. Newer methods employing infrared matrix-assisted laser desorption electrospray ionization (IR-MALDESI)<sup>13</sup> combined with direct visualization of virus<sup>44</sup> (and evaluation of replication-competent status) would improve the ability to detect an association between ART exposure and inducible virus. The method used here, though bioanalytically validated, may overestimate the ART exposure in cells of interest, as interstitial fluid and other cell population would be included in the analysis.<sup>17</sup> The surface area of small intestine gut-associated lymphoid tissue may also be greater than a similar-



sized biopsy of the large intestine.<sup>45</sup> Nonetheless, using a consistent pharmacokinetic assay across tissue samples, normalized by sample weight (and several were within the same individual), the comparative analyses across tissues and ART regimens were consistent with prior reports using different pharmacokinetic assays.<sup>12</sup>

These results add to the current limited data on tissue ART drug concentrations and have potential implications for HIV cure strategies. It is possible that ongoing replication is more likely to occur in lymphoid tissues because of cell-to-cell spread of virus,<sup>46</sup> which may be less efficiently blocked by ART. It is also possible that the higher levels of immune activation in tissues influence ongoing viral replication and/or tissue ART penetration.<sup>6,47</sup> Future studies should measure ART tissue concentrations and viral transcription/replication in lymph nodes (for which we had limited sample to perform PK measures only), and might demonstrate even higher levels of viral transcription in lymph nodes, where we observed lower ART tissue penetration compared to blood or gut. To ascertain whether tissue ART exposure will play an important role in future HIV cure strategies, the influence of drug pressure on viral evolution needs to be further explored using detailed methods to quantify replication-competent virus (such as viral outgrowth assays<sup>48</sup> or assays that closely estimate the frequency of intact virus<sup>49,50</sup>), along with ultra-sensitive single genome viral sequencing.<sup>51</sup> The ability to apply these assays is challenging given the limited number of cells that can be collected from tissue sampling, but would ultimately help guide future strategies aimed at improving ART delivery to tissues,<sup>52</sup> reducing immune activation, and eliminating long-lived HIV-infected cells in key anatomic sites.

## Supplementary Material

Refer to Web version on PubMed Central for supplementary material.

## ACKNOWLEDGEMENTS

The authors wish to acknowledge the participation of all the study participants who contributed to this work as well as the clinical research staff of the UCSF SCOPE cohort who made this research possible.

**FUNDING:** This work was supported in part by the National Institutes of Health (SGD: DARE Collaboratory [U19AI096109], SAL: K23GM112526, RMS: KL2TR000143, SAY: R01DK108349, R01AI132128, ADK and MLC: P30 AI050410), the Foundation for AIDS Research (amfAR), and the Merck Foundation as an investigator-initiated study. The content of this publication does not necessarily reflect the views or policies of the Department of Health and Human Services, nor does mention of trade names, commercial products, or organizations imply endorsement by the U.S. Government. The funders had no role in study design, data collection and analysis, decision to publish, or preparation of the manuscript.

## REFERENCES

1. Deeks SG, Autran B, Berkhout B, et al. Towards an HIV cure: a global scientific strategy. *Nature reviews Immunology* 2012; 12(8): 607–14.
2. Hunt PW. HIV and aging: emerging research issues. *Current opinion in HIV and AIDS* 2014; 9(4): 302–8. [PubMed: 24824891]
3. Legarth RA, Ahlstrom MG, Kronborg G, et al. Long-Term Mortality in HIV-Infected Individuals 50 Years or Older: A Nationwide, Population-Based Cohort Study. *J Acquir Immune Defic Syndr* 2016; 71(2): 213–8. [PubMed: 26334734]

4. Yukl SA, Gianella S, Sinclair E, et al. Differences in HIV burden and immune activation within the gut of HIV-positive patients receiving suppressive antiretroviral therapy. *The Journal of infectious diseases* 2010; 202(10): 1553–61. [PubMed: 20939732]
5. Hatano H, Strain MC, Scherzer R, et al. Increase in 2-Long Terminal Repeat Circles and Decrease in D-dimer After Raltegravir Intensification in Patients With Treated HIV Infection: A Randomized, Placebo-Controlled Trial. *The Journal of infectious diseases* 2013; 208(9): 1436–42. [PubMed: 23975885]
6. Yukl SA, Shergill AK, McQuaid K, et al. Effect of raltegravir-containing intensification on HIV burden and T-cell activation in multiple gut sites of HIV-positive adults on suppressive antiretroviral therapy. *AIDS* 2010; 24(16): 2451–60. [PubMed: 20827162]
7. Dinoso JB, Kim SY, Wiegand AM, et al. Treatment intensification does not reduce residual HIV-1 viremia in patients on highly active antiretroviral therapy. *Proc Natl Acad Sci U S A* 2009; 106(23): 9403–8. [PubMed: 19470482]
8. Gandhi RT, Zheng L, Bosch RJ, et al. The effect of raltegravir intensification on low-level residual viremia in HIV-infected patients on antiretroviral therapy: a randomized controlled trial. *PLoS Med* 2010; 7(8).
9. McMahon D, Jones J, Wiegand A, et al. Short-course raltegravir intensification does not reduce persistent low-level viremia in patients with HIV-1 suppression during receipt of combination antiretroviral therapy. *Clin Infect Dis* 2010; 50(6): 912–9. [PubMed: 20156060]
10. Wang X, Mink G, Lin D, Song X, Rong L. Influence of raltegravir intensification on viral load and 2-LTR dynamics in HIV patients on suppressive antiretroviral therapy. *J Theor Biol* 2017; 416: 16–27. [PubMed: 28025011]
11. Lorenzo-Redondo R, Fryer HR, Bedford T, et al. Persistent HIV-1 replication maintains the tissue reservoir during therapy. *Nature* 2016; 530(7588): 51–6. [PubMed: 26814962]
12. Fletcher CV, Staskus K, Wietgreffe SW, et al. Persistent HIV-1 replication is associated with lower antiretroviral drug concentrations in lymphatic tissues. *Proc Natl Acad Sci U S A* 2014; 111(6): 2307–12. [PubMed: 24469825]
13. Weber MD, Andrews E, Prince HA, et al. Virological and immunological responses to raltegravir and dolutegravir in the gut-associated lymphoid tissue of HIV-infected men and women. *Antivir Ther* 2018.
14. Palmer S, Wiegand AP, Maldarelli F, et al. New real-time reverse transcriptase-initiated PCR assay with single-copy sensitivity for human immunodeficiency virus type 1 RNA in plasma. *J Clin Microbiol* 2003; 41(10): 4531–6. [PubMed: 14532178]
15. Patterson KB, Prince HA, Stevens T, et al. Differential penetration of raltegravir throughout gastrointestinal tissue: implications for eradication and cure. *AIDS* 2013; 27(9): 1413–9. [PubMed: 23945503]
16. Robbins BL, Nelson SR, Fletcher CV. A novel ultrasensitive LC-MS/MS assay for quantification of intracellular raltegravir in human cell extracts. *J Pharm Biomed Anal* 2012; 70: 378–87. [PubMed: 22727807]
17. Mouton JW, Theuretzbacher U, Craig WA, Tulkens PM, Derendorf H, Cars O. Tissue concentrations: do we ever learn? *J Antimicrob Chemother* 2008; 61(2): 235–7. [PubMed: 18065413]
18. Cory TJ, Winchester LC, Robbins BL, Fletcher CV. A rapid spin through oil results in higher cell-associated concentrations of antiretrovirals compared with conventional cell washing. *Bioanalysis* 2015; 7(12): 1447–55. [PubMed: 26168252]
19. Trezza CR, Kashuba AD. Pharmacokinetics of antiretrovirals in genital secretions and anatomic sites of HIV transmission: implications for HIV prevention. *Clin Pharmacokinet* 2014; 53(7): 611–24. [PubMed: 24859035]
20. Thompson CG, Cohen MS, Kashuba AD. Antiretroviral pharmacology in mucosal tissues. *J Acquir Immune Defic Syndr* 2013; 63 Suppl 2: S240–7.
21. Choi SO, Rezk N, Kim JS, Kashuba AD. Development of an LC-MS method for measuring TNF in human vaginal tissue. *J Chromatogr Sci* 2010; 48(3): 219–23. [PubMed: 20223089]
22. Patterson KB, Prince HA, Kraft E, et al. Penetration of tenofovir and emtricitabine in mucosal tissues: implications for prevention of HIV-1 transmission. *Sci Transl Med* 2011; 3(112): 112re4.

23. Yukl SA, Kaiser P, Kim P, et al. HIV latency in isolated patient CD4(+) T cells may be due to blocks in HIV transcriptional elongation, completion, and splicing. *Sci Transl Med* 2018; 10(430).
24. Schacker TW, Nguyen PL, Beilman GJ, et al. Collagen deposition in HIV-1 infected lymphatic tissues and T cell homeostasis. *J Clin Invest* 2002; 110(8): 1133–9. [PubMed: 12393849]
25. Schacker TW, Nguyen PL, Martinez E, et al. Persistent abnormalities in lymphoid tissues of human immunodeficiency virus-infected patients successfully treated with highly active antiretroviral therapy. *J Infect Dis* 2002; 186(8): 1092–7. [PubMed: 12355359]
26. Skarda DE, Taylor JH, Chipman JG, et al. Inguinal lymph node biopsy in patients infected with the human immunodeficiency virus is safe. *Surg Infect (Larchmt)* 2007; 8(2): 173–8. [PubMed: 17437362]
27. Yukl SA, Kaiser P, Kim P, Li P, Wong JK. Advantages of using the QIAshredder instead of restriction digestion to prepare DNA for droplet digital PCR. *Biotechniques* 2014; 56(4): 194–6. [PubMed: 24724845]
28. Mardirossian G, Tagesson M, Blanco P, et al. A new rectal model for dosimetry applications. *J Nucl Med* 1999; 40(9): 1524–31. [PubMed: 10492375]
29. Rizk ML, Hang Y, Luo WL, et al. Pharmacokinetics and pharmacodynamics of once-daily versus twice-daily raltegravir in treatment-naive HIV-infected patients. *Antimicrob Agents Chemother* 2012; 56(6): 3101–6. [PubMed: 22430964]
30. Boffito M, Jackson A, Amara A, et al. Pharmacokinetics of once-daily darunavir-ritonavir and atazanavir-ritonavir over 72 hours following drug cessation. *Antimicrob Agents Chemother* 2011; 55(9): 4218–23. [PubMed: 21709075]
31. Arab-Alameddine M, Lubomirov R, Fayet-Mello A, et al. Population pharmacokinetic modelling and evaluation of different dosage regimens for darunavir and ritonavir in HIV-infected individuals. *J Antimicrob Chemother* 2014; 69(9): 2489–98. [PubMed: 24821595]
32. Savic RM, Barrail-Tran A, Duval X, et al. Effect of adherence as measured by MEMS, ritonavir boosting, and CYP3A5 genotype on atazanavir pharmacokinetics in treatment-naive HIV-infected patients. *Clin Pharmacol Ther* 2012; 92(5): 575–83. [PubMed: 23033116]
33. Wenning L, Rizk M, Luo W, et al. PK/PD Analyses for QDMRK, a Phase III Study of the Safety & Efficacy of Once versus Twice Daily Raltegravir in Treatment-Naive HIV-infected Patients. Abstract O\_09. 12th International Workshop on Clinical Pharmacology of HIV Therapy; 2011 4 13–15.; Miami, FL.; 2011.
34. Elliott JH, McMahon JH, Chang CC, et al. Short-term administration of disulfiram for reversal of latent HIV infection: a phase 2 dose-escalation study. *Lancet HIV* 2015; 2(12): e520–9. [PubMed: 26614966]
35. Evering TH, Mehandru S, Racz P, et al. Absence of HIV-1 evolution in the gut-associated lymphoid tissue from patients on combination antiviral therapy initiated during primary infection. *PLoS Pathog* 2012; 8(2): e1002506. [PubMed: 22319447]
36. Bailey JR, Sedaghat AR, Kieffer T, et al. Residual human immunodeficiency virus type 1 viremia in some patients on antiretroviral therapy is dominated by a small number of invariant clones rarely found in circulating CD4+ T cells. *J Virol* 2006; 80(13): 6441–57. [PubMed: 16775332]
37. Kearney MF, Spindler J, Shao W, et al. Lack of detectable HIV-1 molecular evolution during suppressive antiretroviral therapy. *PLoS Pathog* 2014; 10(3): e1004010. [PubMed: 24651464]
38. Josefsson L, von Stockenström S, Faria NR, et al. The HIV-1 reservoir in eight patients on long-term suppressive antiretroviral therapy is stable with few genetic changes over time. *Proc Natl Acad Sci U S A* 2013; 110(51): E4987–96. [PubMed: 24277811]
39. Wagner TA, McKernan JL, Tobin NH, Tapia KA, Mullins JI, Frenkel LM. An increasing proportion of monotypic HIV-1 DNA sequences during antiretroviral treatment suggests proliferation of HIV-infected cells. *J Virol* 2013; 87(3): 1770–8. [PubMed: 23175380]
40. Kroon E, de Souza M, Chottanapund S, et al. Persistent detection of HIV RNA+ cells with ART started in Fiebig 1&2 vs Fiebig 3–5 Conference on Retroviruses and Opportunistic Infections; 2018; Boston, MA.; 2018.
41. Palmer S, Maldarelli F, Wiegand A, et al. Low-level viremia persists for at least 7 years in patients on suppressive antiretroviral therapy. *Proceedings of the National Academy of Sciences of the United States of America* 2008; 105(10): 3879–84. [PubMed: 18332425]

42. Perelson AS, Essunger P, Cao Y, et al. Decay characteristics of HIV-1-infected compartments during combination therapy. *Nature* 1997; 387(6629): 188–91. [PubMed: 9144290]
43. Rizza SA, Badley AD. HIV protease inhibitors impact on apoptosis. *Med Chem* 2008; 4(1): 75–9. [PubMed: 18220972]
44. Deleage C, Wietgreffe SW, Del Prete G, et al. Defining HIV and SIV Reservoirs in Lymphoid Tissues. *Pathog Immun* 2016; 1(1): 68–106. [PubMed: 27430032]
45. Helander HF, Fandriks L. Surface area of the digestive tract - revisited. *Scand J Gastroenterol* 2014; 49(6): 681–9. [PubMed: 24694282]
46. Sherer NM, Lehmann MJ, Jimenez-Soto LF, Horensavitz C, Pypaert M, Mothes W. Retroviruses can establish filopodial bridges for efficient cell-to-cell transmission. *Nat Cell Biol* 2007; 9(3): 310–5. [PubMed: 17293854]
47. Massanella M, Esteve A, Buzon MJ, et al. Dynamics of CD8 T-cell activation after discontinuation of HIV treatment intensification. *Journal of acquired immune deficiency syndromes* 2013; 63(2): 152–60. [PubMed: 23392458]
48. Eriksson S, Graf EH, Dahl V, et al. Comparative analysis of measures of viral reservoirs in HIV-1 eradication studies. *PLoS pathogens* 2013; 9(2): e1003174. [PubMed: 23459007]
49. Bruner KM, Murray AJ, Pollack RA, et al. Defective proviruses rapidly accumulate during acute HIV-1 infection. *Nat Med* 2016; 22(9): 1043–9. [PubMed: 27500724]
50. Procopio FA, Fromentin R, Kulpa DA, et al. A Novel Assay to Measure the Magnitude of the Inducible Viral Reservoir in HIV-infected Individuals. *EBioMedicine* 2015; 2(8): 872–81.
51. Boltz VF, Rausch J, Shao W, et al. Ultrasensitive single-genome sequencing: accurate, targeted, next generation sequencing of HIV-1 RNA. *Retrovirology* 2016; 13(1): 87. [PubMed: 27998286]
52. Mandal S, Kang G, Prathipati PK, Fan W, Li Q, Destache CJ. Long-acting parenteral combination antiretroviral loaded nano-drug delivery system to treat chronic HIV-1 infection: A humanized mouse model study. *Antiviral Res* 2018; 156: 85–91. [PubMed: 29885378]

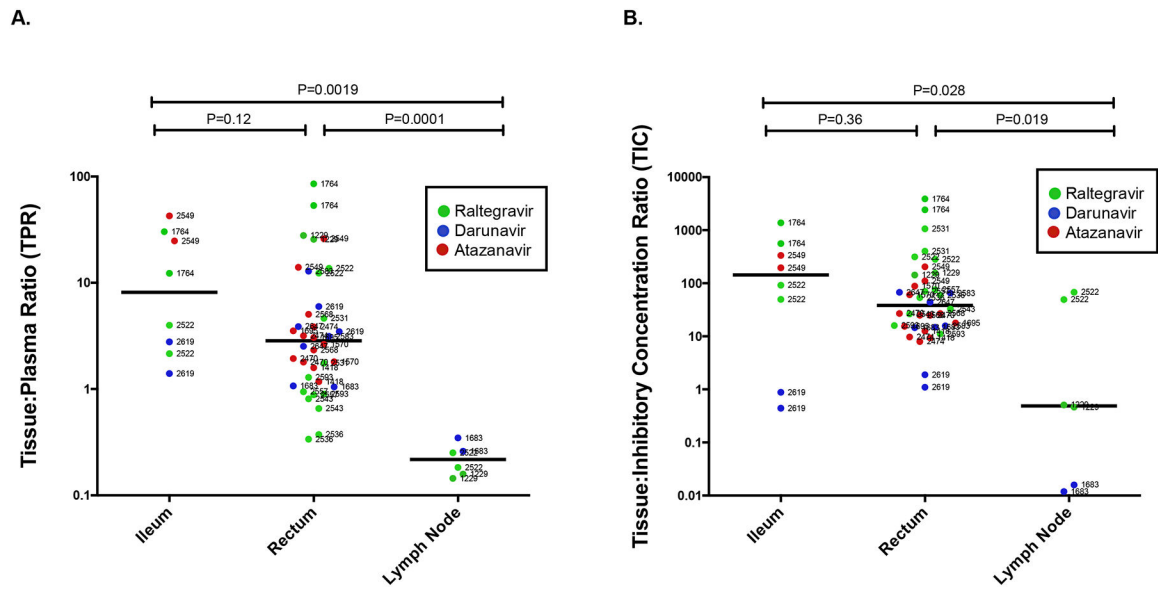
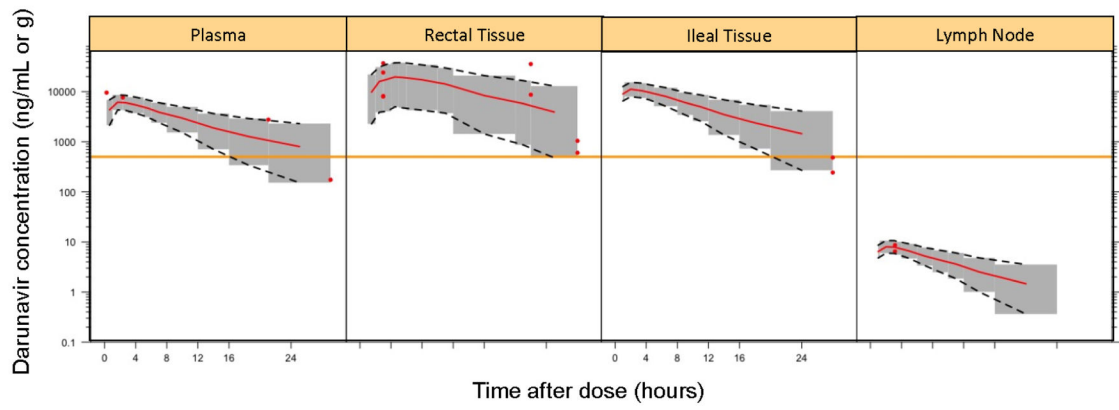
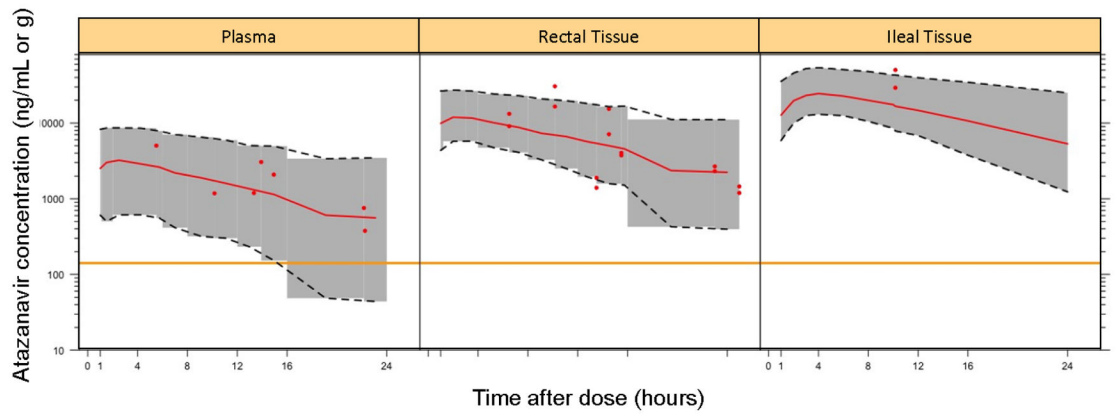


**Figure 1.** Tissue PK for each biologic duplicate (marked by study participant ID number) are shown by tissue type (ileum, rectum, and lymph node). Individual dots represent unique biologic duplicates, with medians shown as horizontal black bars. Tissue:plasma penetration ratios (TPRs) were calculated as the ratio of antiretroviral therapy (ART) concentrations in tissue (ng/g converted ng/mL) to plasma (ng/mL) (A).<sup>8</sup> Ratios >1 indicate that the drug concentrates in tissue, whereas ratios <1 indicate concentrations in tissue are lower than in plasma. Tissue:inhibitory concentration ratios (TICs) were calculated as the ratio of antiretroviral therapy (ART) concentrations in tissue (ng/g) to previously reported drug-specific *in vivo* inhibitory concentrations in plasma (ng/mL) (A).<sup>28,29</sup> Ratios >1 indicate that the drug concentrates in tissue were higher than previously reported inhibitory concentrations.

**A.**



**B.**



C.

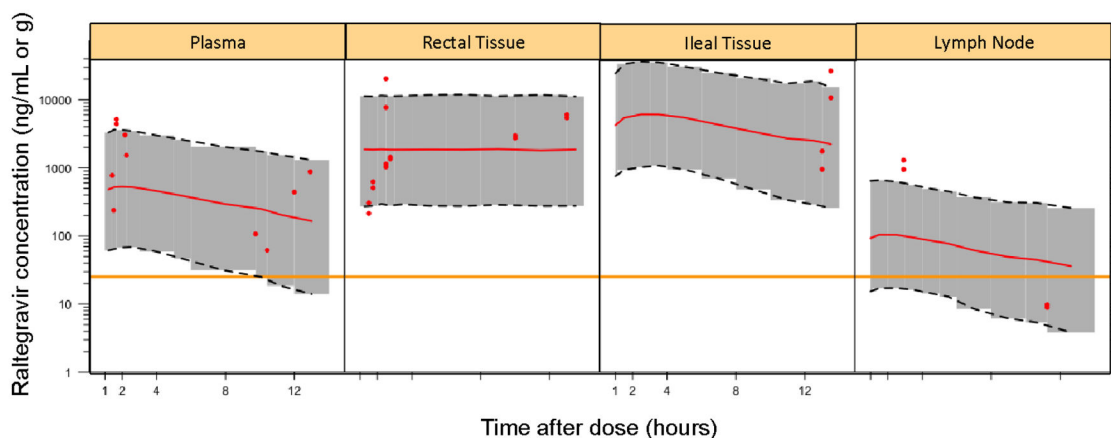


**Figure 2.** Visual Predicted Check (VPC) showing simulated darunavir (DRV), atazanavir (ATV), and raltegravir (RAL) concentrations over time in plasma, rectal, ileal, and lymph node tissues from the final PK model. Simulated medians are shown as red lines, 90% prediction intervals are shown as gray shaded regions, and the target concentrations are shown as the orange horizontal lines (below which clinical virologic failure was observed in clinical trials).<sup>28,29</sup> Observed duplicate data are shown as red dots.

**Table 1.**

Negative binomial regression estimates of the multiplicative effect of PK (rectal tissue:plasma penetration ratio)<sup>8</sup> [TPR] on copies of HIV (per million rectal cells) (A) and on HIV RNA/DNA ratios (B).

<b>A) HIV transcripts</b>	<b>N</b>	<b>Fold-change per 2-fold increase in TPR<sup>a</sup></b>	<b>P</b>
Readthrough RNA	18	1.00 (0.33, 3.06)	1.00
TAR RNA	20	0.68 (0.34, 1.33)	0.26
Long LTR RNA	20	0.12 (0.01, 1.54)	0.10
Nef RNA	20	0.28 (0.01, 6.25)	0.42
PolyA RNA	20	0.27 (0.02, 4.02)	0.34
Tat-Rev RNA <sup>b</sup>	20	0.02 (0.00, 49.83)	0.32
Long LTR DNA	38	1.02 (0.58, 1.80)	0.93
<b>B) HIV RNA/DNA ratios</b>	<b>N</b>	<b>Fold-change per 2-fold increase in TPR<sup>a</sup></b>	<b>P</b>
Readthrough RNA/Long LTR DNA	18	1.41 (0.72, 2.75)	0.31
TAR RNA/Long LTR DNA	20	0.34 (0.08, 1.43)	0.14
Long LTR RNA/Long LTR DNA	20	<b>0.22 (0.05, 0.97)</b>	<b>0.046</b>
Nef RNA/Long LTR DNA	20	0.38 (0.07, 1.92)	0.24
PolyA RNA/Long LTR DNA	20	0.39 (0.12, 1.26)	0.12
Tat-Rev RNA/Long LTR DNA	20	0.24 (0.03, 2.22)	0.21

<sup>a</sup>Fold-change in HIV copies or fold-change in HIV RNA/DNA ratio per 2-fold increase in tissue:plasma penetration ratio (TPR) with 95% confidence intervals.

<sup>b</sup>Estimates for copies of tat-rev were unstable, because the majority of values were zero (75%ile = 0 copies, mean 0.63 copies, and standard deviation = 1.4 copies).



**Table 2.**

Negative binomial regression estimates of the multiplicative effect of PK (rectal tissue: inhibitory concentration ratio<sup>28,29</sup> [TIC]) on copies of HIV (per million rectal cells) (A) and on HIV RNA/DNA ratios (B).

A) HIV transcripts	N	Fold-change per 2-fold increase in TIC <sup>a</sup>	P
Readthrough RNA	18	<b>0.56 (0.34, 0.93)</b>	<b>0.026</b>
TAR RNA	20	0.55 (0.26, 1.21)	0.14
Long LTR RNA	20	<b>0.25 (0.09, 0.76)</b>	<b>0.014</b>
Nef RNA	20	<b>0.20 (0.04, 0.96)</b>	<b>0.044</b>
PolyA RNA	20	0.31 (0.06, 1.62)	0.17
Tat-Rev RNA <sup>b</sup>	20	0.02 (0.00, 11.44)	0.22
Long LTR DNA	38	0.76 (0.53, 1.08)	0.13
B) HIV RNA/DNA ratios	N	Fold-change per 2-fold increase in TIC <sup>a</sup>	P
Readthrough RNA/Long LTR DNA	18	0.87 (0.60, 1.26)	0.45
TAR RNA/Long LTR DNA	20	0.80 (0.37, 1.73)	0.56
Long LTR RNA/Long LTR DNA	20	<b>0.36 (0.15, 0.86)</b>	<b>0.021</b>
Nef RNA/Long LTR DNA	20	0.35 (0.11, 1.13)	0.080
PolyA RNA/Long LTR DNA	20	0.56 (0.23, 1.36)	0.20
Tat-Rev RNA/Long LTR DNA	20	0.07 (0.00, 3.08)	0.17

<sup>a</sup>Fold-change in HIV copies or fold-change in HIV RNA/DNA ratio per 2-fold increase in tissue:inhibitory concentration ratio (TIC) with 95% confidence intervals.

<sup>b</sup>Estimates for copies of tat-rev were unstable, because the majority of values were zero (75% ile = 0 copies, mean 0.63 copies, and standard deviation = 1.4 copies).

**Table 3.**

Negative binomial regression estimates of antiretroviral therapy (ART) regimen (protease inhibitor [PI] versus integrase inhibitor [INI]) on copies HIV transcripts (per million rectal cells) (A) and on HIV RNA/DNA ratios (B).

A) HIV Transcripts	PI (N)	INI (N)	Fold-Change for PI vs. INI <sup>a</sup>	P
Readthrough RNA	14	4	<b>3.02 (1.06, 8.56)</b>	<b>0.038<sup>b</sup></b>
TAR RNA	14	6	<b>5.40 (1.78, 16.36)</b>	<b>0.0029</b>
Long LTR RNA	14	6	4.55 (0.98, 21.14)	0.053
Nef RNA	14	6	<b>6.92 (1.06, 45.17)</b>	<b>0.043</b>
PolyA RNA	14	6	2.70 (0.32, 22.53)	0.36
Tat-Rev RNA <sup>c</sup>	14	6	--	--
Long LTR DNA	22	16	1.40 (0.73, 2.70)	0.31
B) HIV RNA/DNA Ratios	N		Fold-Change for PI vs. INI <sup>a</sup>	P
Readthrough RNA/Long LTR DNA	14	4	1.32 (0.58, 3.03)	0.51
TAR RNA/ Long LTR DNA	14	6	3.76 (0.95, 14.91)	0.060
Long LTR RNA LTR/Long LTR DNA	14	6	4.04 (0.93, 17.54)	0.063
Nef RNA/Long LTR DNA	14	6	5.00 (0.96, 24.93)	0.055
PolyA RNA/Long LTR DNA	14	6	1.81 (0.41, 7.89)	0.43
Tat-Rev RNA/Long LTR DNA <sup>c</sup>	14	6	--	--

<sup>a</sup>Fold-change in HIV copies or HIV RNA/DNA ratio for PI- vs. INI-based ART with 95% confidence intervals.

<sup>b</sup>Estimates for readthrough RNA are based on <5 samples in the INI group and should thus be interpreted with caution.

<sup>c</sup>Estimates for copies of tat-rev did not converge; the majority of values were zero (75<sup>th</sup>ile = 0 copies, mean 0.63 copies, and standard deviation = 1.4 copies)